Fabrication and optical characterization of GaN quasi-phase matching crystal by double polarity selective area growth in metal organic vapor phase epitaxy

Functional Materials Letters
Vol. 1, No. 1 (2015) 1–4

FABRICATION AND OPTICAL CHARACTERIZATION OF GAN QUASI-PHASE MATCHING CRYSTAL BY DOUBLE POLARITY SELECTIVE AREA GROWTH IN METAL ORGANIC VAPOR PHASE EPITAXY

Kai Matsuhisa[1], Hiroki Ishihara[1], Mako Sugiura[2], Yoshimasa Kawata[3,4], Atsushi Sugita[2], Yoku Inoue[1], Takayuki Nakano[1,3*]

[1]*Department of Electronics and Materials Science, Shizuoka University, 3-5-1 Johoku, Hamamatsu 432-8561, Japan*

[2]*Department of Applied Chemistry and Biochemical Engineering, Shizuoka University, 3-5-1 Johoku, Hamamatsu, Shizuoka 432-8561, Japan*

[3]*Research Institute of Electronics, Shizuoka University, 3-5-1 Johoku, Hamamatsu 432-8011, Japan*

[4]*Department of Mechanical Engineering, Shizuoka University, 3-5-1 Johoku Hamamatsu, Shizuoka 432-8561, Japan*

**nakano.takayuki@shizuoka.ac.jp*

Received Day Month Year; Revised Day Month Year

The fabrication of ultra-violet (UV) second-harmonic-generation (SHG) (UV-SHG) devices requires GaN quasi-phase matching (GaN-QPM) crystals with periodically arranged polar GaN. For fabricating GaN-QPM crystals, the double polarity selective area growth (DP-SAG) using carbon mask technique is employed. However, the growth of narrow (2–4 µm) pitch pattern GaN-QPM crystals, which is necessary for UV-SHG devices, has not been reported using this technique. Herein, we report the successful fabrication of 4-µm pitch pattern GaN-QPM. We fabricated a thick GaN-QPM crystal at the optimized V/III ratio. Through optical characterization, we observed SHG generation from the GaN-QPM crystal fabricated using DP-SAG.

Keywords: Gallium nitride (GaN), quasi-phase matching (QPM) crystal, selective area growth, metal-organic vapor phase epitaxy(MOVPE)

Group-III nitride semiconductors are useful in various applications including short wavelength applications owing to their wide bandgap of up to 6.1 eV. [1, 2] Several areas where these materials are employed include: blue light emitting diodes (LEDs)[3, 4], blue light laser diodes (LDs),[5-7] solar cells,[8] high voltage high-electron-mobility-transistors (HEMTs),[9-11] and radiation detectors.[12,13] Recently, group-III nitride semiconductors have also attracted significant attention for their application in optical devices in the UV region.

The stable GaN crystal structure is a wurtzite structure, which is characterized by an asymmetry along the *c*-axis. The structure in combination with the strong ionic characteristic of the composition results in a large spontaneous polarization. Although the bandgaps, refractive indices, and wave numbers for these different polar faces are the same, the sign of the tensors expressing their second-order nonlinear susceptibilities and the direction of spontaneous polarization are opposite.[14-16] Using these features, it has become possible to fabricate Quasi Phase Matching (QPM) crystals by arranging each polar GaN periodically.[17] Wavelength conversion by QPM crystal facilitates the generation of light with half wavelength of that of fundamental light. GaN-QPM crystals are capable of wavelength conversion into the near UV range by SHG, as GaN has a wide wavelength transparency range owing to its wide bandgap.[17] Moreover, $Al_xGa_{1-x}N$ allows us to convert into wavelengths including the UV-C (deep ultra violet) range by SHG.[18-21] Such GaN-based SHG devices are expected to be applicable as novel optical devices in the UV region.[22] Many studies have reported the fabrication process of GaN- or AlGaN-QPM crystals.[17-23]

The conventional technique for fabricating GaN-QPM crystal involves several iterations of a growth process and a necessary intermediate etching process. Alternatively, double polar selective area growth (DP-SAG) using carbon mask has been proposed and developed for the fabrication of GaN-

QPM crystals, which requires only one growth process.[24-26] DP-SAG is able to reduce the growth steps, such as taking out the wafer from the chamber for selective area growth; this is because the carbon mask can be removed easily in the chamber. Therefore, using DP-SAG for fabrication of GaN-QPM crystal reduces the growth time and simplifies the growth process. Fabrication of 20-μm pitch pattern of GaN-QPM crystals has been reported using DP-SAG.[26]

For SHG, the following equation is well known:[17, 27]

$$\Lambda = \frac{m_{QPM}\lambda_{\omega}}{2(n_{2\omega}-n_{\omega})} \qquad (1)$$

where m_{QPM} is phase matching order number, λ_{ω} is incident wavelength, $n_{2\omega}$ is effective refractive index at SHG, and n_{ω} is effective refractive index at incident wavelength. As per the equation, the incident wavelength (λ_{ω}) is proportional to the pitch pattern (Λ).

For wavelength conversion by SHG in the UV region, narrow (2~4 μm) pitch pattern GaN-QPM crystal is necessary. However, the fabrication of 4 μm pitch pattern GaN-QPM crystal is difficult when using the growth conditions employed for 20 μm pitch pattern GaN-QPM crystal. In this study, we attempt to fabricate 4 μm pitch pattern GaN-QPM crystal using the DP-SAG process with abrupt hetero-interface for UV-SHG devices.

SHG characterization for GaN-QPM crystal was evaluated using maker fringe measurement with variable incidence angles. Our measurements showed that the second harmonic was generated at the 3rd, 5th, 7th, and 9th phase-matching order number conditions in the 4-μm pitch GaN-QPM crystal.

GaN-QPM crystal was fabricated using metal organic vapor phase epitaxy (MOVPE) with ammonia (NH_3) as the N source and trimethylgalium (TMGa) as the Ga source. The DP-SAG process is carried out as per the following steps: i) first, amorphous-carbon (a-carbon) mask is patterned on Al_2O_3 (0001) substrate using the liftoff process; ii) then, an initial Ga-polar GaN layer is grown on the masked free region of the patterned substrate for 10 min; iii) next, NH_3 treatment is performed to remove the carbon mask and allow the nitridation of the Al_2O_3 substrate in the region that was blocked by the mask; iv) next, for the continuous layer growth of initial N-polar GaN, initial DP-GaN is grown at N-polar GaN optimum growth condition; v) subsequently, a GaN-QPM crystal layer is grown on the substrate. During this process, Ga-polar GaN grew on the initial Ga-polar GaN layer and N-polar GaN grew on the nitridated Al_2O_3 substrate where an (000-1) AlN layer had formed by the nitridation of Al_2O_3. Steps (ii)–(iv) were performed during a single MOVPE growth process. A schematic of the process and a time chart are shown in Ref. 26.

GaN-QPM crystal was grown on a c-Al_2O_3 by DP-SAG process under the following growth conditions: growth temperature was 1050 ºC, growth pressure was 100 Torr, total gas flow rate was 2600 sccm, NH_3 flow rate was 500, 1000, and 1200 sccm. TMGa flow rate was varied between 3.0 μmol/min and 5.54 μmol/min, V/III ratio was varied between 7400 and 11300.

For structural evaluation, scanning electron microscopy (SEM) and atomic force microscopy (AFM) were used for observing the surface morphology and cross-sectional structure of the GaN-QPM crystal. A Kelvin force microscope (KFM) and KOH etching were used to determine the polarity of GaN-QPM crystal. Different KOH resolvability between Ga polar GaN and N polar GaN were used for KOH etching, and different surface electrical potentials were used for KFM.[28-30]

For optical characterization, maker fringe measurement was used. The incident laser was a Ti:Al_2O_3 laser (center wavelength of 780 nm, pulse width of 100 fs and frequency of 75 MHz). The light power was varied between 50 mW and 275 mW. The transmission wavelength of 390 nm was measured through a low-pass filter using a photo-multiplier tube. At the peak angle, the wavelength profile was measured for evaluating the transmission wavelength.

The formation of initial layer of double polarity GaN (DP-GaN) is important for the 4 μm pitch pattern GaN-QPM crystal with abrupt hetero-interface. Hence, it is crucial to study the surface morphology and this was done using AFM. Ga-polar GaN initial layer was grown for the formation of Ga-polar region in step (ii) of the DP-SAG process. Ga-polar GaN was grown on the unmasked region, and no layer was grown in the masked region. A flow rate of 500 sccm of NH_3 and 3.0 μmol/min of TMGa flow were used for growing an initial Ga-polar GaN layer.

Figure 1 shows (a) AFM image, (b) AFM cross sectional profile of an initial Ga-polar GaN layer. In Fig. 1(a), periodical Ga-polar GaN growth region and carbon mask region is observed. In Fig. 1(b), the cross-sectional profile shows that the thickness of Ga-polar GaN is about 250 nm and shows the formation of a pitch pattern of 4 μm. These results indicate successful formation of periodical Ga-polar GaN initial layer with 4 μm pitch.

After Ga-polar GaN initial layer growth, NH_3 cleaning was performed for removing carbon mask and nitriding the substrate on the carbon mask region. For the formation of N-polar region, a DP-GaN initial layer was grown. Again, during the initial layer growth of DP-GaN, AFM was used to confirm the formation of each polar GaN region. In this step, flow rates of 1000 sccm of NH_3 and 3.92 μmol/min of TMGa were used.

The AFM image and cross-sectional profile of the fabricated DP-GaN initial layer are shown in Fig. 1(c) and Fig. 1(d), respectively. In Fig. 1(c), a periodical arrangement of different surface morphology was observed. This result indicates that the continuous layer which is different from Ga-polar GaN is grown on the carbon mask region. In Fig. 1(d), each polar GaN can be seen to have approximately the same thickness. In addition, the thickness of Ga-polar GaN is hardly increased. This result suggests that the pitch width is shorter than the surface diffusion length of the Ga precursor, so that it flows into the N-polar region and contributes to the lateral growth of Ga-polar GaN and the growth of N-polar GaN. In DP-SAG, controlling the growth of each polar GaN layer to the same thickness is important, because preventing the Ga or N-polar GaN overgrowth to the other polar region is possible. These results indicate that fabrication of DP-GaN initial layer is achieved for GaN-QPM crystal. 4 μm pitch pattern GaN-QPM crystal was fabricated by growing each polar GaN epitaxial layer on DP-GaN initial layer.

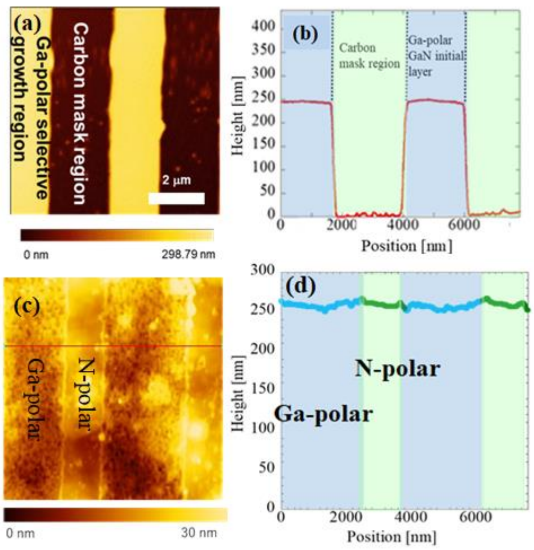

Fig. 1. (a) AFM image of Ga-polar GaN initial layer, (b) AFM cross-sectional image of Ga polar GaN initial layer, (c) AFM image of each polar GaN initial layer, and (d) AFM cross sectional image of each polar GaN initial layer.

For the fabrication of GaN-QPM crystal, each polar GaN epitaxial layer was grown with the following conditions: V/III ratio: 9600, growth time: 50 min, and growth temperature: 1050 ^{o}C. This optimized growth condition is a condition in which the growth rate of Ga-polar GaN is slightly faster than the that of N-polar by adjusting the V/III ratio based on Ref. 25. Figure 2 shows surface SEM images (a) before KOH etching, (b) after KOH etching, and AFM images (c) before KOH etching, and (d) after KOH etching.

In Figs. 2(a) and 2(c), a periodical pattern of different surface morphology in a 4 μm pitch pattern was observed because of different surface morphologies for each polar GaN. In Figs. 2(b) and 2(d), periodical etching in 4 μm pitch pattern was observed. This result suggests the formation of periodic polarity GaN, as the Ga-polar region did not etch, whereas the N-polar region was etched by KOH. Therefore, these results indicate that 4 μm pitch pattern GaN-QPM with periodical polar arrangement was fabricated successfully using DP-SAG.

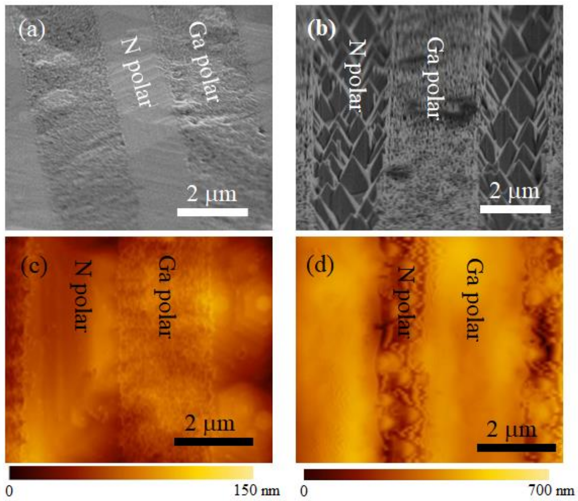

Fig. 2. (a) Surface SEM image before KOH etching, (b) surface SEM image after KOH etching, (c) AFM image before KOH etching, (d) AFM image after KOH etching of GaN-QPM crystal fabricated at V/III ratio of 9600.

Furthermore, we also fabricated and investigated a thick GaN-QPM crystal. Figure 3 shows cross sectional SEM images of thick GaN-QPM crystal (a) before KOH etching, and (b) after KOH etching. Figure 3 (a) shows that no voids were formed at the hetero-interface. In Fig. 3(b), GaN-QPM crystal can be seen periodically etched, and vertical hetero-interfaces fabricated. These results indicate that 5-μm-thick GaN-QPM crystal with vertical hetero-interface was fabricated using DP-SAG.

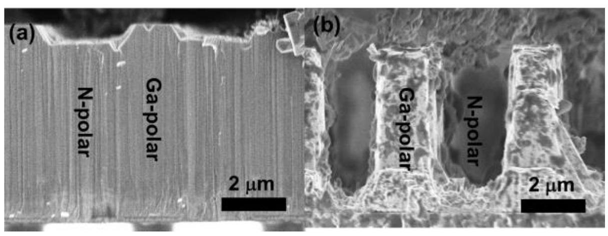

Fig. 3. (a) Surface SEM image before KOH etching, (b) surface SEM image after KOH etching of thick GaN-QPM crystal.

In the maker fringe measurement in which the substrate is rotated with respect to the incident light, the effective pitch width Λ_θ changes according to $\Lambda_\theta = \Lambda/\sin\theta$ depending on the incident angle θ. Therefore, following eq. (1), peak angle θ

can be derived from Λ (pitch width for GaN-QPM crystal) and Λ_θ (pitch width for SHG). Figure 4 (a) shows the maker fringe measurement result. In Fig. 4 (a), three peaks are observed at 20, 32, and 51°. Each peak position corresponds to the theoretical peak positions at each phase matching order number (7, 5, and 3, respectively). Figure 4 (b) shows the relationship between incident light power and peak intensity. In Fig. 4(b), peak intensity is proportional to the square of incident light power. Figure 4(c) shows the relationship between phase matching order number and each peak intensity at 275 mW. In Fig. 4(c), the reciprocal square root of peak intensity is proportional to the phase matching order number. As the SHG peak intensity is proportional to the square of incident light power and peak intensity is inversely proportional to the square of phase matching order number,[31] these results indicate that each peak is due to the peak of SHG.

Figure 4(d) shows the wavelength spectrum measurement of the peak on third phase matching order and the incident light for 780 nm. In Fig. 4(d), the SHG peak of 390 nm, corresponding to half the wavelength of that of the incident light, was observed. However, the conversion efficiency showed a quite low value of 2.17×10^{-8} %. The reason for the low conversion efficiency could be due to the short transmission length because of the oblique incident angle to the GaN-QPM crystal. In order to achieve higher conversion efficiency, longer transmission lengths are needed to increase the number of conversions, which can be achieved by producing horizontal waveguide structures. These results indicate that second harmonic could be generated from GaN-QPM crystal by DP-SAG.

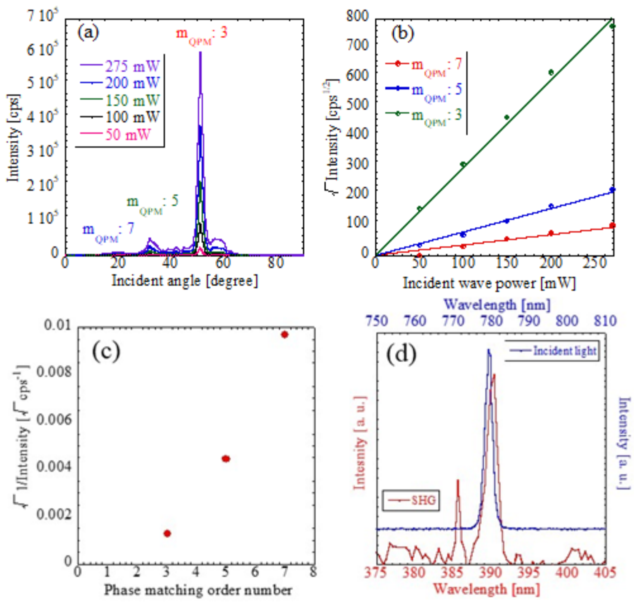

Fig. 4. (a) Maker fringe analysis results, (b) the graphical relationship between incident energy and peak intensity at each peak position, (c) the graphical relationship between phase matching order number and peak intensity at 275 mW, and (d) wavelength spectrum results at the angle on third phase matching order.

In this study, we report the optimized growth condition of the 4 μm pitch pattern GaN-QPM crystal with abrupt hetero-interface and its optical characteristics. In order to fabricate the GaN-QPM crystal, each polar GaN was grown on DP-GaN initial layer. The fabrication of 4 μm pitch pattern and 5 μm thickness GaN-QPM crystal with abrupt hetero-interface was achieved with DP-SAG optimized conditions. In the optical characterization of the GaN-QPM crystal produced by DP-SAG, the SHG peak was seen at 390 nm. These results indicated that the wavelength conversion from 780 nm to 390 nm was achieved using a GaN-QPM crystal via DP-SAG.

References

1) J. Li, K. Nam *et al.*, Appl. Phys. Lett. **83**, 5163 (2003).
2) I. Vurgaftman *et al.*, J. Appl. Phys. **89**, 5815 (2001).
3) S. Nakamura *et al.*, Jpn. J. Appl. Phys. **32**, L8 (1993).
4) T. Mukai *et al.*, Jpn. J. Appl. Phys. **37**, L839 (1988).
5) M. Funato *et al.*, Jpn. J. Appl. Phys. **45**, L659 (2006).
6) S. Nakamura *et al.*, Jpn. J. Appl. Phys. **35**, L74 (1996).
7) K. Okamoto *et al.*, Jpn. J. Appl. Phys. **46**, L820 (2007).
8) S. Nagahama *et al.*, Jpn. J. Appl. Phys. **40**, 3075 (2001).
9) O. Jani *et al.*, Appl. Phys. Lett. **91**, 132117 (2007).
10) M. Asif Khan *et al.*, Appl. Phys. Lett. **63**, 1214 (1993).
11) Y. Dora *et al.*, IEEE Electron Devices Lett. **27**, 713 (2006).
12) K. Atsumi *et al.*, APL Mater. **2**, 032106 (2014).
13) M. Sugiura *et al.*, Jpn. J. Appl. Phys. **55**, 05FJ02 (2016).
14) O. Ambacher *et al.*, J. Appl. Phys. **85**, 3222 (1999).
15) M. Stutzmann *et al.*, Phys. Status Solidi B **228**, 505 (2001).
16) F. Bernardini *et al.*, Phys. Rev. B **56**, R10024 (1997)
17) A. Chowdhury *et al.*, Appl. Phys. Lett. **83**, 1077 (2003).
18) D. Alden *et al.*, Appl. Phys. Lett. **114**, 103504 (2019).
19) D. Alden *et al.*, Appl. Phys. Lett. **108**, 261106 (2016).
20) R. Kirste *et al.*, Appl. Phys. Lett. **102**, 181913 (2013).
21) M. P. Hoffmann *et al.*, Phys. Status Solidi A **212**, 1039 (2015).
22) C. Xiong *et al.*, Opt. Express **19**, 10462 (2011).
23) J. Hite *et al.*, Opt. Mater. Express **2**, 1203 (2012).
24) Y. Fujita *et al.*, Jpn. J. Appl. Phys. **52**, 08JB26 (2013).
25) K. Kuze *et al.*, Jpn. J. Appl. Phys. **55**, 05FA05 (2016).
26) H. Yagi *et al.*, Phys. Status Solidi B **255**, 1700475 (2018).
27) R. Katayama *et al.*, Proc. of SPIE 2012, 8268 (2012).
28) H. M. Ng *et al.*, Jpn. J. Appl. Phys. **42,** L1405 (2003).
29) H. Matsumura *et al.*, Appl. Phys. Express **2,** 101001 (2009).
30) R. Katayama *et al.*, J. Cryst. Growth **301-302**, 447 (2007).
31) A. Yariv, Optical Electronics 272. Harcourt Brace Jovanovich College Publishers (1991).